Kochi Chapter

Indian Geotechnical Conference
IGC 2022
15th – 17th December, 2022, Kochi

Influence of Density on the Dynamic Properties of IntactRock Masses

Sakshi Rohilla[1] and Resmi Sebastian[2]

[1] Research Scholar, Department of Civil Engineering, Indian Institute of Technology Ropar, Ropar-140001, India
[2] Assistant Professor, Department of Civil Engineering, Indian Institute of Technology Ropar, Ropar-140001, India
2018cez0007@iitrpr.ac.in, resmi@iitrpr.ac.in

Abstract. The determination of dynamic properties of geomaterials is essential from the point of view of many geotechnical engineering problems subjected to dynamic loading. The density of the geomaterial plays a vital role in deciding the dynamic properties and Poisson's ratio of the material. In the present study, resonant column apparatus has been used for the laboratory testing of intact gypsum material to identify the influence of density on the dynamic properties of Poisson's ratio of rocks. The experimental results showed that the unconfined compressive strength of the material increases exponentially with increased density. The reduction in the Poisson's ratio and material damping ratio and a rise in the dynamic modulus have been observed with an increase in the density of the material. Furthermore, with the rise in the strain amplitude, the value of Poisson's ratio and damping ratio increases, and the modulus value decreases. The study attempted to establish the correlation between the density and the dynamic properties of the material under varying strain amplitudes.

Keywords: Resonant Column testing, density, dynamic properties, Poisson's ratio, strain amplitude.

1 Introduction

Rock mechanics and dynamic loading associated with rocks hold a vital role in many mining, energy, petroleum, environmental, and civil engineering applications. The awareness of the dominance of dynamic loading on the reflexive behaviour of rock masses is vitally crucial in the design and safety evaluation of structures constructed in them. Deere and Miller (1966) studied the behaviour of various types of rocks and predicted that the elastic modulus of rock increases linearly with an increase in the dry density. Yilmaz and Yuksek (2009) studied the behaviour of gypsum and anticipated that the elastic modulus increases logarithmically with a decrease in the porosity of gypsum. The previous studies reported that the wave velocity hikes with an escalation in the density of the rock mass (Christensen and Salisbury (1975); Kahraman and Yeken (2008); Rahmouni et al. (2013)). The resonant column apparatus (RCA) has been extensively used to investigate the dynamic response of geomaterials at varying strain amplitudes and other experimental conditions. H. B. Seed & Idriss, 1970 and Meng & Rix, 2003 investigated the nonlinear response of geomaterials under dynamic

loading conditions. Kumar and Madhusudan (2010) performed a study to elucidate the effect of confining pressure and density on the Poisson's ratio of the soils. Researchers have performed many studies on gypsum plaster using resonant column apparatus, considering it as a model material (Fratta and Santamarina (2001); Cha et al. (2009); Md Nordin et al. (2015); A. Perino (2015); Sebastian & Sitharam (2015, 2016, and 2018). Anderson (1974), Hardin (1972), and Darendeli (2001) provided models to analyse the nonlinear response of soils and rocks. In the present study, the influence of density on the dynamic properties of the model material, gypsum, has been explored. The influence of material density on the Poisson's ratio over a range of strain amplitudes has been investigated. Furthermore, a modified hyperbolic model has been used to develop a normalized modulus reduction curve.

2 Materials and methodology

2.1 Materials and sample preparation

In this study, resonant column (RC) testing was performed on the cylindrical gypsum plaster samples having diameters and heights of 50 mm and 100mm respectively, using the resonant column apparatus (RCA) supplied by GDS instruments, London, UK. Gypsum can be categorized as a naturally occurring crystalline sedimentary rock, which, when heated at a temperature of ~150° C, provides Plaster of Paris (POP). When POP comes in contact with moisture, turns to gypsum again. The testing specimens were prepared by mixing a specific amount of water and POP, filling the mixture into the split mould, and letting it dry for a few hours before extrusion. The density of the gypsum plaster sample produced by mixing POP and water depends on the consistency of the POP and water mix. In this study, many cylindrical gypsum plaster specimens were prepared under varying POP and water proportions to perform unconfined compressive strength (UCS) and resonant column (RC) testing.

2.2 Testing technique and measurements of dynamic properties in shear and flexure

The fundamental essence of RC testing is to apply vibrations to a cylindrical specimen in its fundamental mode of vibration. The specimen is vibrated for a range of frequency values, and their response in terms of strain amplitude is observed; the frequency complementary to the maximum response amplitude is called resonant frequency. The wave velocities of the specimen in the shear and flexure can then be obtained by collating the resonant frequency with the apparatus and material characteristics.
In the RC test, a sinusoidal excitation in terms of shear and flexure is applied at the top of the cylindrical specimen using an electromagnetic drive system connected to the specimen. The net excitation at the topmost end of the testing cylindrical specimen is applied using a magnet-coil arrangement which is provided at the four arms of the driving plate, as shown in fig.1. The arrangement of the magnet-coil system is provided in such a way that whenever current passes through the magnet-coil driving system, a magnetic field is produced, which gives rise to oscillatory motion in the driving plate.
A set of four magnets are banded together in series to introduce a net rotational force to the topmost end of the cylindrical specimen. For the implementation of flexural

vibrations, a net horizontal force is exerted at the top of the cylindrical specimen employing two alternate magnets, as shown in fig.1.

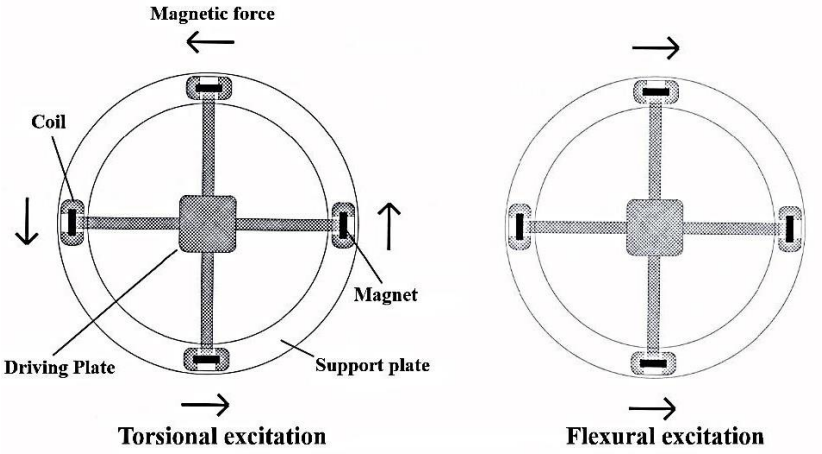

Fig. 1 Simplified view of load application at the top of the specimen

2.3 Measurement of strain amplitude for shear and flexure

Torsional strain is quantified by employing the angle of twist of the testing cylinder. Torsional strain varies across the radius of the test specimen, from zero at the central axis to some limited value (maximum value) at the outer surface of the cylinder (Hall, Richard, and Woods, 1970). The level of torsional strain is estimated from the accelerometer measurements in terms of amplitude, the resonant frequency of the specimen, and the specimen geometry. An accelerometer is attached at the top of the cylindrical specimen to read the response of the specimen upon the action of particular vibrational loading in the form of angular acceleration. The displacement of the accelerometer, $\gamma_{measured}$ related to the angular acceleration, a, can be written as:

$$a = \omega^2 * \gamma_{measured} \quad (1)$$

Therefore, the displacement of the accelerometer at resonance can be written as:

$$\gamma_{measured} = \frac{9.81 * V}{4\pi^2 * f^2} = \frac{0.2485 * V}{f^2} \quad (2)$$

Where $\omega = 2\pi f$; (f is the resonant frequency), V is the voltage recorded by the accelerometer (Volts).

The angle of twist produced in the specimen can be obtained simply by considering the cylindrical geometry of the specimen (i.e., $\theta = \gamma_{measured}$ /L), therefore:

$$\theta = \frac{0.2485 * V}{0.04325 * f^2} = \frac{5.7454 * V}{f^2} \quad (3)$$

Where 0.04325m is the accelerometer's offset from the rotation axis.

Finally, the shearing strain for solid cylindrical specimens using the standard GDS RCA drive mechanism can be given as:

$$\gamma = \frac{0.8 * R * \theta}{L} = \frac{4.596 * V * R}{f^2 * L} \quad (4)$$

Where, R is the radius, and L is the cylinder (m) length.

Cascante et al. (1998) adopted Rayleigh's method to investigate the deflection in the material under the first mode of flexural vibration. They considered a cantilever beam under a fixed-free flexural vibration system, where additional masses placed at the free end of the cantilever beam, to obtain the value of flexural modulus (E). The flexural modulus of the material is related to the resonant frequency as:

$$\omega_f^2 = \frac{33}{140} \frac{3 * E * I_b}{L^3 * \left[* m_s + \sum_{i=1}^{N} (m_i * f_i) \right]} \quad 5$$

Where ω_f is the flexural resonant frequency in the first mode, f_i is equivalent height, whose relation with the top ($h1_i$) and bottom ($h0_i$) heights of the mass m_i is provided in Equation 6, m_s, L, E, I_b are the mass, height, Young's modulus, area moment of inertia of the testing cylindrical specimen about the longitudinal axis, respectively.

$$f_i = 1 + \frac{3(h0_i + h1_i)}{2 * L} + \frac{3(h1_i^2 + h0_i h1_i + h0_i^2)}{4 * L^2} \quad 6$$

In cases of flexural excitation, the shape of the deflection curve created when a specimen is loaded is directly proportional to the flexural strain exerted on it. For the cylindrical specimen with radius R and length L, the average strain can be defined as:

$$\varepsilon_{avg} = \frac{4}{\pi} RL\alpha \quad 7$$

Where, the value of α is the flexural displacement measured at the x_{accel} elevation of the accelerometer. Substituting the value of $\gamma_{measured}$ from equation 2, the displacement of the accelerometer at resonance can be written as:

$$\varepsilon_f = \frac{4 * 0.2489 * V * R}{\pi * (f_n^2 * L * [2L + 3(x_{accel} - L])} = \frac{0.3164 * V * R}{(f_n^2 * L * [2L + 3(x_{accel} - L])} \quad 8$$

Where x_{accel} is the upstanding distance from the base of the testing cylindrical specimen to the centre of the accelerometer. For the standard GDS RCA, the value of x_{accel} is 0.005m from the top surface of the specimen top-cap and is therefore 0.055m from the base of the sample top-cap.

In the RC test, the material damping ratio, D, is computed by employing the free vibration decay pattern. This outline is obtained using the measurements of the accelerometer framed on the driving plate to gather the response of testing material upon loading. A sinusoidal wave strikes the cylindrical specimen, and the response of the column under the influence of a single strike is extracted in the form of displacement amplitude (ASTM-4015, 1992; Madhusudan and Kumar, 2013). The amplitudes of two successive peaks are used to identify the material damping ratio. The ratio of the logarithm of two successive amplitudes demonstrates the logarithmic decrement value, δ. The value of δ can be identified by plotting the logarithm of amplitude versus the number of cycles (n) graph. The material damping ratio, D, in terms of δ, can be expressed as:

$$\delta = \frac{1}{n} log_e \frac{z_1}{z_{n+1}} = \frac{2\pi D}{\sqrt{1 - D^2}} \quad 9$$

Where z_1, z_2, and z_{n+1} are the amplitudes corresponding to the first, second, and $(n+1)^{th}$ cycle, respectively.

3 Analysis and discussions

3.1 Influence of density on static unconfined compressive strength

The unconfined compressive strength of intact gypsum plaster at various densities was inspected under dry conditions by pursuing the following standards, i.e., ASTM D3148-02 2002, ISRM 1979, ISRM 1985. Fig. 2 presents the variation of unconfined compressive strength (UCS) of gypsum plaster with density (ρ). The tests were performed thrice for each density of gypsum plaster, and an average strength was noted. The static unconfined compressive strength rose exponentially with an escalation in density.

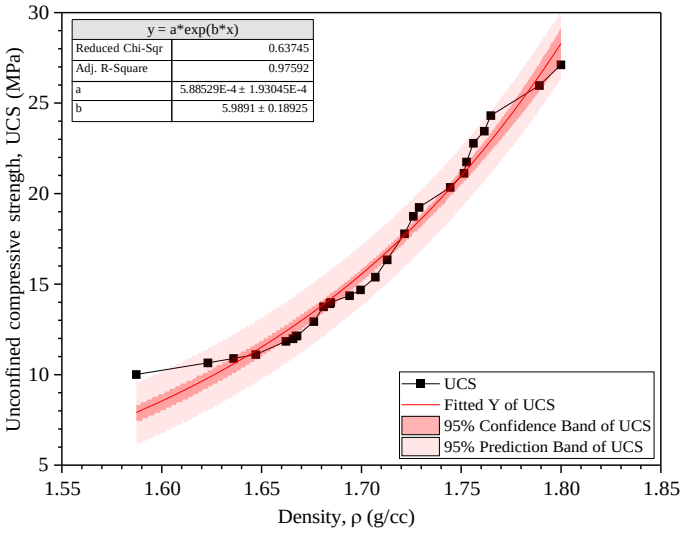

Fig.2 Density versus unconfined compressive strength of gypsum plaster

3.2 Influence of density on the dynamic properties of gypsum plaster

A varying range of density has been adapted to investigate the eminence of intact specimens on the dynamic properties. In this study, the densities of 1.575 g/cc, 1.6 g/cc, 1.65 g/cc, , 1.7 g/cc, 1.75 g/cc, and 1.8 g/cc have been used. The resonant column testing of all the six representative densities has been performed over a range of strain amplitudes to obtain the wave velocities in shear and flexure and material damping ratio in shear and flexure. The values of both the shear wave velocity and flexure wave velocity were observed to rise with an escalation in the density of the specimen and fall with a hike in the strain amplitude. The damping ratio values in shear and flexure were observed to fall with a rise in the density and hike with an escalation in the strain amplitude values, as shown in Figs. 3 and 4. The shear and flexural moduli of all the specimens were obtained from the corresponding wave velocities over a range of strain levels. Likewise, in the wave velocities, the moduli of the specimens were found to rise with the density, as presented in Tables 1 and 2.

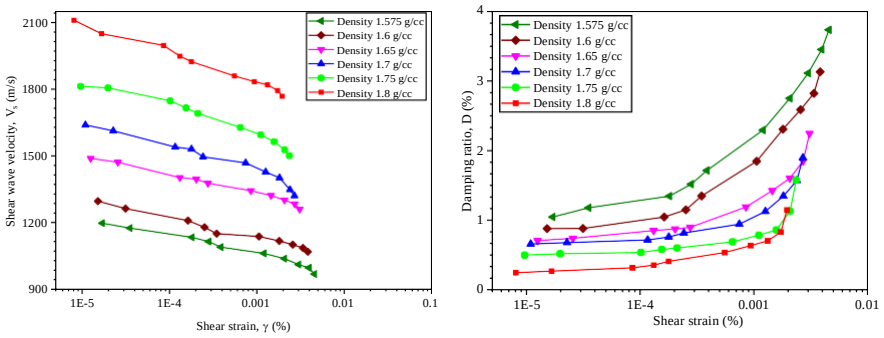

Fig. 3 Shear wave velocity and damping ratio in shear versus strain amplitudes

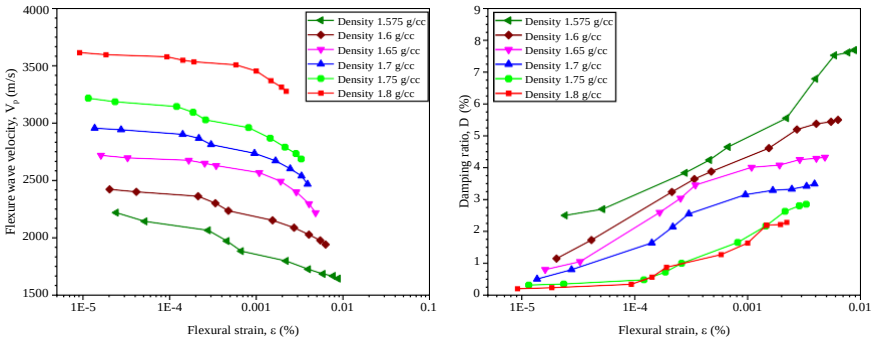

Fig. 4 Flexure wave velocity and damping ratio in flexure versus strain amplitudes

Table 1 Shear modulus of gypsum plaster at varying density values

Shear strain amplitude (%)	**Shear Modulus (GPa) Density (g/cc)**					
	1.575	**1.6**	**1.65**	**1.7**	**1.75**	**1.8**
$1*10^{-5}$	3.000	3.346	4.068	4.779	5.548	6.794
$5*10^{-5}$	2.826	3.221	3.960	4.575	5.407	6.559
$1*10^{-4}$	2.895	3.187	3.923	4.524	5.294	6.413
$5*10^{-4}$	2.606	2.988	3.713	4.313	5.032	6.055
$1*10^{-3}$	2.347	2.964	3.644	4.243	4.934	5.934

Table 2 Flexure modulus of gypsum plaster at varying density values

Flexural strain amplitude (%)	**Flexure Modulus (GPa) Density (g/cc)**					
	1.575	**1.6**	**1.65**	**1.7**	**1.75**	**1.8**
$1*10^{-5}$	5.601	6.228	7.425	8.552	9.865	11.708
$5*10^{-5}$	5.329	6.140	7.334	8.480	9.722	11.629
$1*10^{-4}$	5.275	6.112	7.313	8.429	9.658	11.569
$5*10^{-4}$	4.849	5.718	7.213	8.062	9.184	11.480
$1*10^{-3}$	4.627	5.623	7.010	7.897	8.985	11.173

3.4 Influence of density on the Poisson's ratio

The shear and flexural wave velocities, i.e., V_s and V_p can be utilized to obtain the Poisson's ratio of intact gypsum specimens using the expression (Richart et al. 1970).

$$p = \frac{(0.5V_p^2 - V_s^2)}{(V_p^2 - V_s^2)} \quad (10)$$

In this study, the Poisson's ratio has been examined at different densities and strain amplitudes values. The variations of Poisson's ratio at varying strain amplitudes and density levels are shown in Fig. 5. It was noticed that the Poisson's ratio values decrease with an increase in the density of the gypsum plaster specimens and increase continuously with the rise in the values of strain amplitude. The overall values of Poisson's ratio at different densities range from 0.249 to 0.332, corresponding to maximum and minimum density values. As it was clear from the above findings that the Poisson's ratio is a function of strain amplitude and density, a multiple linear regression analysis has been performed. The expression for the analysis is shown in equation 11. The findings of regression analysis are provided in Table 3.

$$p = C * \rho^a * \theta^b \quad (11)$$

Where p is the Poisson's ratio, ρ is the density of gypsum plaster in g/cc, θ is the strain amplitude in %, a is the density exponent, b is the strain exponent, and C is the constant depending on the material type.

Fig. 4 shows the actual and predicted value of Poisson's ratio at different density and strain amplitude levels.

Table 3 Results obtained from the regression analysis performed for Poisson's ratio

Constant c	Coefficient a	Coefficient b	R^2
-0.1904	-1.0955	0.0232	0.97

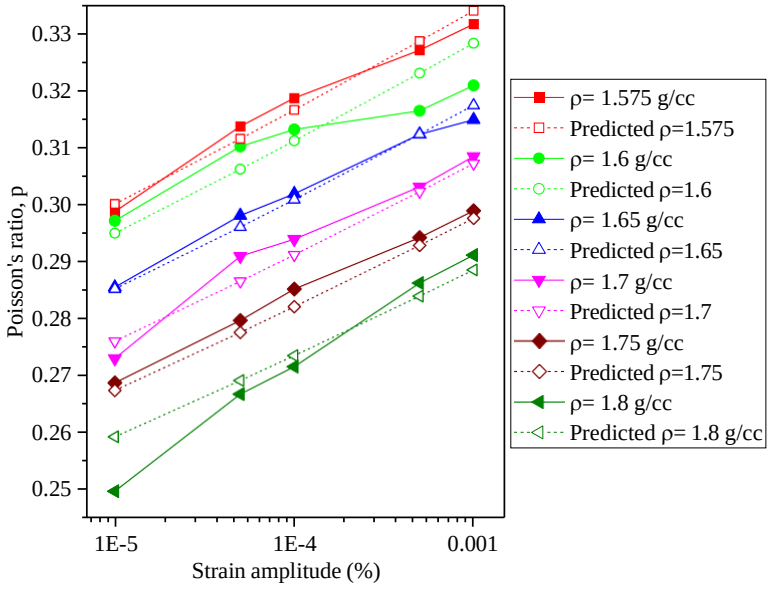

Fig. 5 Poisson's ratio dependence on density and strain amplitude

3.5 Normalized shear modulus reduction curve

Many studies on the geomaterials predicted that the dynamic shear modulus, G, declines, and the material damping ratio, D, rises with the hike in the shear strain

amplitudes (e.g., Bolton Seed & Idriss, 1970; Seed et al. 1986; Darendeli, 2001). The hyperbolic model (Hardin, 1972) and modified hyperbolic model (Darendeli, 2001) are widely adopted to identify the nonlinear response of the geomaterials. The expression for the modified hyperbolic model can be stated as:

$$\frac{G}{G_{max}} = \frac{1}{1 + \left(\frac{\gamma}{\gamma_y}\right)^{\alpha}} \qquad 12$$

Where γ_y is the reference shear strain, whose value corresponds to the G/Gmax value of 0.5.

This study used a modified hyperbolic model to study the nonlinear modulus reduction of gypsum plaster. Fig. 6 shows the pattern of the shear modulus of gypsum plaster with an increase in the strain level obtained from the laboratory testing and the predicted values obtained from the modified hyperbolic model. The findings of the regression assessment performed for the modified hyperbolic model are given in Table 4.

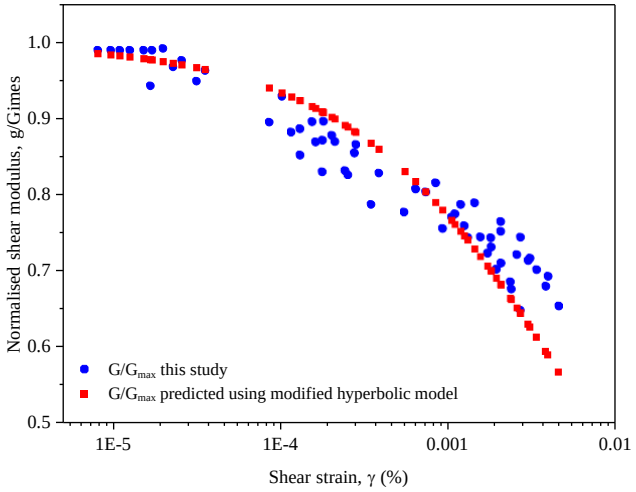

Fig. 6 Normalized modulus reduction curve versus strain

Table 4. Curve fitting parameters of G/G_{max} for the modified hyperbolic model

γ_{ref} (%)	α	R^2
$7.024*10^{-3}$	0.626	0.97

3.6 Dynamic increase factor

Dynamic increase factor (DIF) for different densities of gypsum plaster has been determined by comparing the dynamic modulus (in flexure) with the static modulus (in compression). The DIF values of the intact gypsum plaster for varying densities are reported in Fig. 7. In general, it has been noticed by many researchers that the dynamic increase factor raises with a hike in the strain rate. In this study, the analysis has been performed under a specific narrow range of strain rates. The strain rate corresponding to static unconfined compressive strength test and dynamic resonant column testing is of the order of 10^{-4}/s and 10^{0}/s, respectively. From Fig. 7, it can be noticed that the magnitude of the dynamic increase factor falls from 2.1 to 1.2, with the rise in the density value

from 1.575 g/cc to 1.8 g/cc. The correlation equation of DIF for gypsum plaster corresponding to varying densities is shown in Fig. 7.

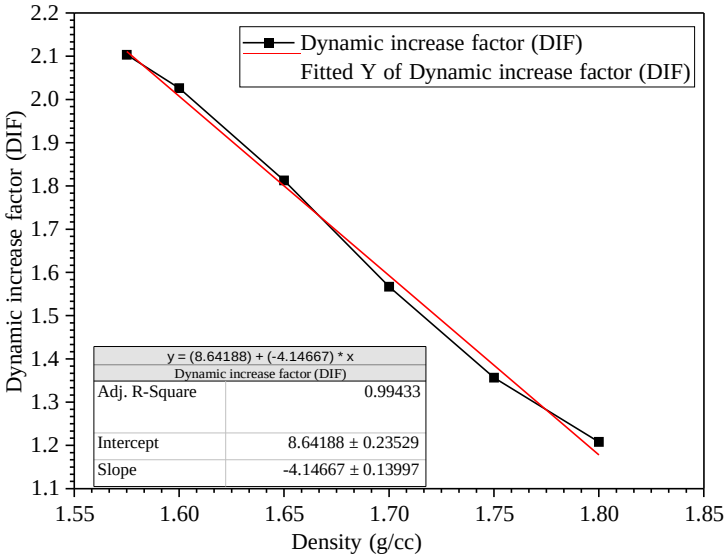

Fig. 7

4 Conclusions

The study has been performed to identify the eminence of density on the UCS and the dynamic properties of intact rock. For the experimentation, a model material, i.e., gypsum plaster, has been used as it is easy to be replicated. To obtain the response, a range of densities of gypsum plaster specimens were tested, and it was found that the UCS of the gypsum plaster hikes exponentially with a rise in the density values. The impact of material density on the dynamic properties has been investigated by performing resonant column testing over a range of strain amplitudes. It was elucidated from the performed testing that there was a declination in the Poisson's ratio and material damping ratio values and a rise in the dynamic modulus with an escalation in the density of the material. Furthermore, the investigation of the influence of strain amplitude on the Poisson's ratio revealed that the magnitude of Poisson's ratio increases logarithmically with the rise in the strain level, and the same trend was observed for all the tested densities. The correlation between the density and the dynamic increase factor (DIF) elucidated that the DIF values reduce linearly with an increase in the density values.

References

1. Anderson, D.G. and Woods, R.D. (1975). "Comparison of Field and Laboratory Moduli," Proceedings, In Situ Measurement of Soil Properties, ASCE, Vol. 1, Raleigh, NC, pp. 66-92.

2. ASTM International, ASTM D 3148-02, 2002. Standard Test Method for Elastic Moduli of Intact Rock Core Specimens in Uniaxial Compression. West Conshohocken, PA 19428-2959, United States.

3. ASTM International, ASTM D 4015−92, 2000. Standard test methods for modulus and damping of soils by resonant column method, Annual book of ASTM Standards. West Conshohocken, PA: ASTM.

4. Cascante, G., Vanderkooy, J., and Chung, W., 2003, Difference between current and voltage measurements in resonant – column testing. Canadian Geotechnical Journal, 40 (4), 806–820. doi:10.1139/t03-023

5. Cha, M., Cho, G., and Santamarina, JC, 2009, Long wavelength P-wave and S-wave propagation in jointed rock masses. Geophysics, 74 (5), E205–E214. doi:10.1190/1.3196240

6. Christensen, N.J., Salisbury, U.H., 1975. Structure and constitution of the lower oceanic crust. Rev. Geophys. Space Phys. 13, 57086.

7. Darendeli, M. B. (2001). "Development of a New Family of Normalized Modulus Reduction and Material Damping Curves." Ph.D. Dissertation, the University of Texas at Austin, 362p.

8. Deere D. and Miller R. (1966): "Engineering classification and index properties for intact rock" Tech. Report No AFWL - TR-65-116, Air Force Weapons Lab., Kirtland Air Base, New Mexico. doi.org/10.1080/17486025.2016.1139753

9. Fratta, D. and Santamarina, J.C., 2002, Shear wave propagation in jointed rock: state of stress. Géotechnique, 52 (7), 495–505. doi:10.1680/geot.2002.52.7.495

10. Hardin, B. O. (1972). "Shear modulus and damping in soil: Measurement and parameter effects." Article in ASCE Soil Mechanics and Foundation Division Journal. June 1972. https://www.researchgate.net/publication/275030013.

11. ISRM (1985). International Society of Rock Mechanics Commission on testing methods, suggested method for determining point load strength. Int J Rock Mech Min Sci Geomech Abstr 22:51–60

12. ISRM (1979). Suggested methods for determining water content, porosity, density, absorption, and related properties and swelling and slake-durability index properties. International Society for Rock Mechanics, Commission on Standardization of Laboratory and Field Tests. Int. J. Rock Mech. Min. Sci. Geomech. Abstr. 16, 145–156.

13. Kahraman, S., Yeken, T., 2008. Determination of physical properties of carbonate rocks from P-wave velocity. Bull. Eng. Geol. Environ. 67, 277–281.

14. Kumar, J. & Madhusudhan, B.N. (2010). Effect of relative density and confining pressure on Poisson ratio from bender and extender elements tests. Geotechnique 60, No7, 561-567.

15. Madhusudhan, B.N., Kumar, J., 2013. Damping of sands for varying saturation. J. Geotech. Geoenviron. Eng. (ASCE)139(9),1625–1630.

16. Meng, J., & Rix, G. J. (2003). "Reduction of equipment-generated damping in resonant column measurements." Géotechnique 53(5):503-512. DOI:10.1680/geot.2003.53.5.503.

17. Mohd-Nordin, M.M., et al., 2014. Long–wavelength elastic wave propagation across naturally fractured rock masses. Rock Mechanics and Rock Engineering, 47, 561–573.doi:10.1007/s00603-013-0448-x

18. Perino, A. and Barla, G., 2015. Resonant column apparatus tests on intact and jointed Rock Specimens with numerical modelling validation. Rock Mechanics and Rock Engineering, 48, 197–211. doi:10.1007/s00603-014-0564-2

19. Rahmouni, A., Boulanouar, A., Boukalouch, M., G_eraud, Y., Samaouali, A., Harnafi, M., Sebbani, J., 2013. Prediction of porosity and density of calcarenite rocks from P-wave velocity measurements. Int. J. Geosci. 4, 1292–1299.

20. Richart, F.E. Jr., Woods, R.D., and Hall, J.R. Jr., 1970. Vibrations of soils and foundations. New Jersey: Prentice Hall.

21. Sebastian, R., & Sitharam, T. G. (2015). "Long Wavelength Propagation of Elastic Waves Across Frictional and Filled Rock Joints with Different Orientations: Experimental Results." Geotechnical and Geological Engineering, 33(4), 923–934. https://doi.org/10.1007/s10706-015-9874-8

22. Sebastian, R., & Sitharam, T. G. (2016). "Long-wavelength propagation of waves in jointed rocks - study using resonant column experiments and model material." Geomechanics and Geoengineering, 11(4), 281–296.

23. Sebastian, R., & Sitharam, T. G. (2018). "Resonant Column Tests and Nonlinear Elasticity in Simulated Rocks." Rock Mechanics and Rock Engineering, 51(1), 155–172. doi.org/10.1007/s00603-017-1308-x

24. Seed, H. B. Wong, R. T., Idriss, I. M. and Tokimatsu, K. (1986) "Moduli and Damping factors for Dynamic Analyses of Cohesionless Soil," J. of Geotech.l Engr., ASCE, Vol. 112, No. GT11, pp. 1016- 103

25. Seed, H. B., Idriss, I. M., Shannon & Wilson., & Agbabian-Jacobsen Associates. (1970). "Soil moduli and damping factors for dynamic response analyses." University of California Berkeley Structural Engineers and Mechanics, NTIS No. PB197869, California University, Berkeley, [Report No. EERC70-10], p.48.

26. Yilmaz, I., Yuksek, G., 2009. Prediction of the strength and elasticity modulus of gypsum using multiple regression, ANN, and ANFIS models. Int. J. Rock Mech. Min. Sci. 46, 803–810.